# Chemistry of Oxo-Sugars. III.[1] Transformations of 2- and 3-Oxoglycosides in a Pyridine Solution[2]

Hong-Min LIU[3] and Yoshisuke TSUDA*

*Faculty of Pharmaceutical Sciences, Kanazawa University, 13-1 Takara-machi, Kanazawa 920, Japan.*
Received August 7, 1995; accepted September 16, 1995

**Methyl *arabino*-hexopyranosid-2-uloses rearranged, in pyridine, into *arabino*-hexopyranosid-3-uloses through an intramolecular hydride shift. The product further isomerized, through enolization, to the most stable *ribo*-hexopyranosid-3-uloses, which, on prolonged standing in the same solvent, gradually liberated methanol giving rise to dioxo derivatives. The last change was particularly evident for 3-oxoglycosides carrying a 4-axial hydroxyl group.**

**Key words** 2-oxoglycoside; hydride shift; 3-oxoglycoside; $^{13}$C-NMR; pyridine; enolization

Although oxo derivatives of glycosides, so-called oxoglycosides, are biologically important in carbohydrate metabolism,[4] very little is known about their chemistry, because of the difficulty of their selective synthesis, as well as their high susceptibility to solvation, and their instability particularly to bases. For example, Theander[5] reported that the oxoglucosides (**1b**, **3a**, **3b**) decomposed in 1.6% lime-water very rapidly (*e.g.*, with a half-life of *ca.* 1 min for **1b**) following the scheme shown in Chart 1 to give the dioxo derivative (**12**). However, the reaction was too rapid to allow definitive identification of the intermediary species or characterization of the reaction path.

Since various oxoglycosides of definite regio- and stereochemistry are now available in pure states,[1] systematic chemical investigation of oxoglycosides is possible. In a previous paper,[1] we clarified the forms of various oxoglycosides existing in solutions (pyridine and water). In this paper we discuss in detail the processes involved in the conversions of 2- and 3-oxoglycosides in pyridine.

Eleven methyl 2- or 3-oxoglycosides, all of which have been reported previously[1,6] (**1**—**8** in Chart 2)[7] were used in this investigation. Pyridine-$d_5$ was chosen as a basic medium, because in such a weak base, the reaction may be retarded, so that the intermediary species would be spectroscopically identifiable.

**Isomerization of 2-Oxoglycosides. Me α-D-*arabino*-2-OG (1a)** The $^{13}$C-NMR spectrum of **1a** in pyridine-$d_5$ showed a complex pattern, when observed immediately after dissolution.[1] However, it converged, after 1—2 h, into the spectrum of a single compound assignable as the oxo form (Fig. 1(1)-a). Further storage in the same solvent resulted in a gradual change of the spectrum, exhibiting peaks of new compound (A), which reached a maximum after 2 d at 27 °C (56% of the total, Fig. 1(1)-b). These peaks then disappeared with a corresponding increase in those of another species (B), which reached a maximum after a week (Fig. 1(1)-c) and was stable for a further several weeks at 27 °C. The spectra of compounds A and B were identical with those of Me α-D-*arabino*-3-OG (**2a**) and Me α-D-*ribo*-3-OG (**3a**), respectively, showing the transformation path **1a**→**2a**→**3a**.

Obviously, **2a** is not a product formed from the enediol intermediate (**9a**), since **9a** produces **3a** as the thermodynamically stable isomer, thus implying that **2a** is the product of an intramolecular hydride shift of 3α-H in **1a** to the 2α-position in **2a**.

In order to prove the hydride shift mechanism, the rearrangement of **1a** in pyridine-$d_5$ containing $D_2O$ was then examined, since the product(s) from the enediol intermediate (**9a**) should lose H at C-2, while those formed by the hydride shift should retain H at that position. The spectrum (Fig. 1(2))[8] showed that **2a** observed in the mixture after 46 h retained 60% of hydrogen at C-2, while C-2 in **3a** was completely replaced by deuterium. The loss of 40% of H at C-2 (40% incorporation of D) in **2a** indicates a partial contribution of the enediol intermediate (**9a**) which is formed from either **1a** or **2a** (see below).

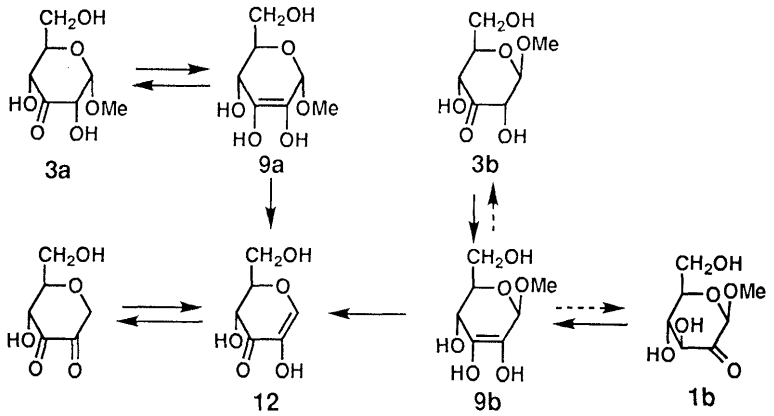


Chart 1

* To whom correspondence should be addressed.

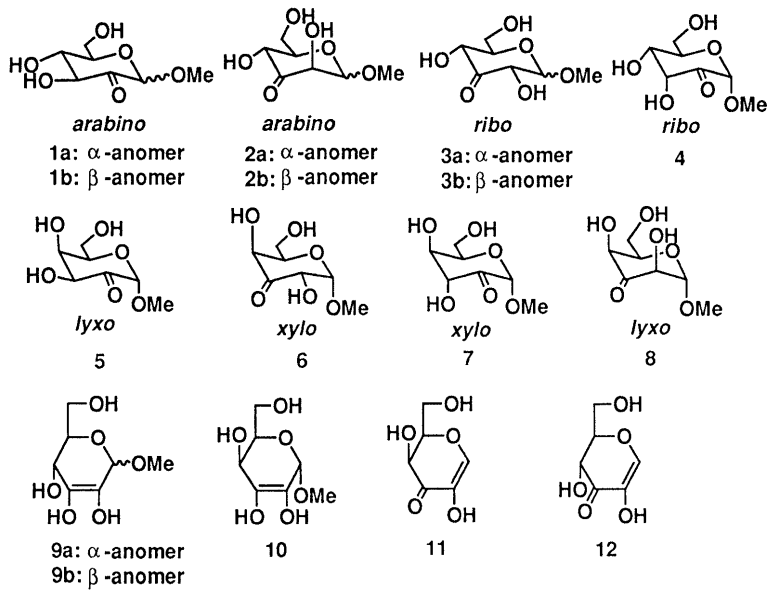


Chart 2

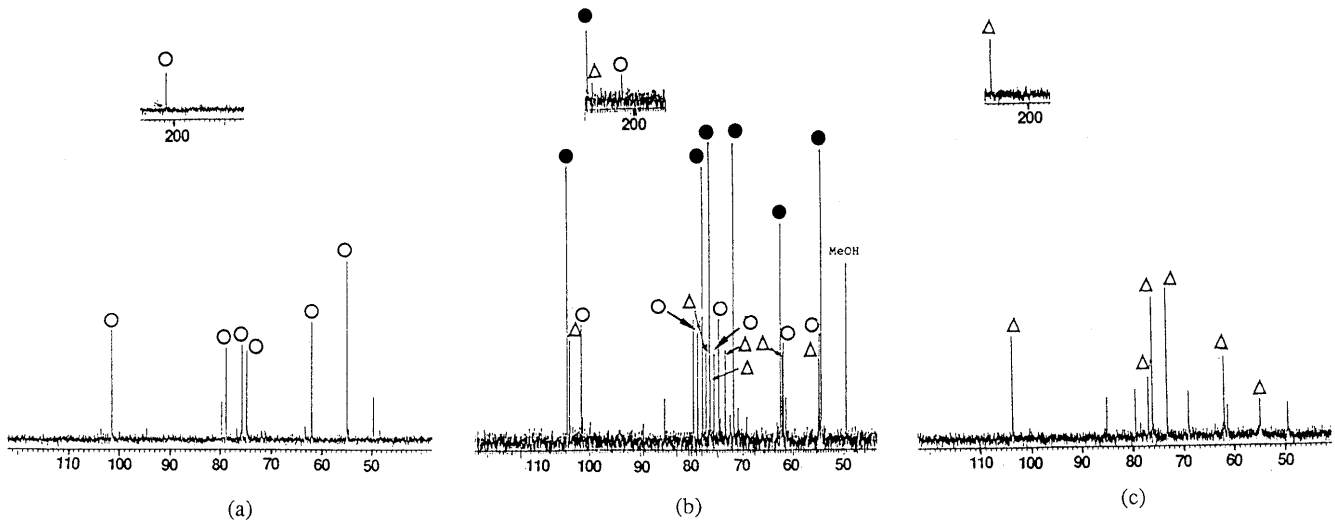


Fig. 1(1). $^{13}$C-NMR Changes of Me α-D-*arabino*-2-OG (**1a**) in Pyridine-$d_5$

(a): after 2 h, (b): after 2 d, (c): after 7 d. ○, Me α-D-*arabino*-2-OG (**1a**); ●, Me α-D-*arabino*-3-OG (**2a**) (A); △, Me α-D-*ribo*-3-OG (**3a**) (B).

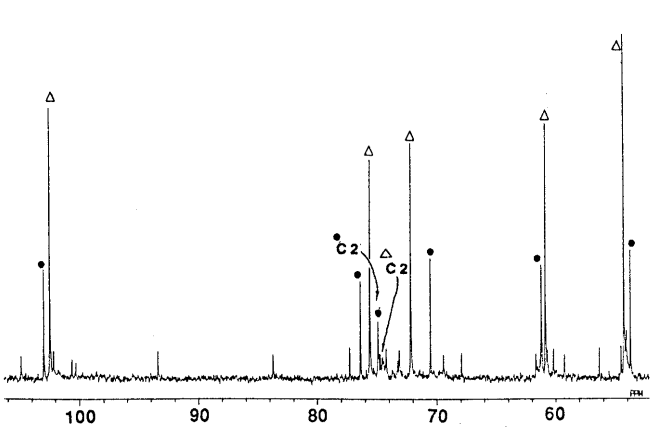


Fig. 1(2). $^{13}$C-NMR Changes of Me α-D-*arabino*-2-OG (**1a**) in Pyridine-$d_5$–$D_2O$ (after 46 h)

●, Me α-D-*arabino*-3-OG (**2a**); △, Me α-D-*ribo*-3-OG (**3a**).

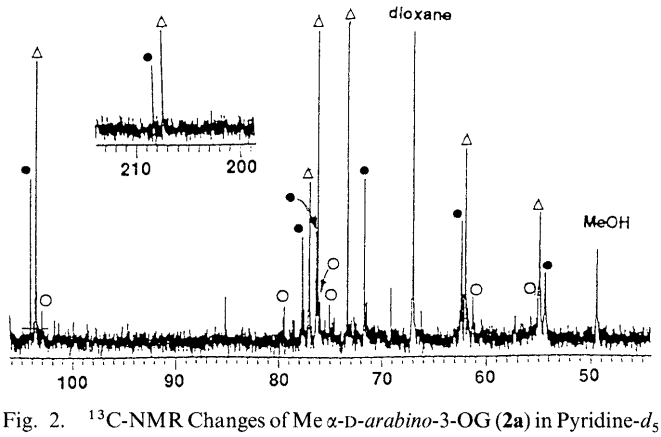


Fig. 2. $^{13}$C-NMR Changes of Me α-D-*arabino*-3-OG (**2a**) in Pyridine-$d_5$ (after 48 h)

○, Me α-D-*arabino*-2-OG (**1a**); ●, Me α-D-*arabino*-3-OG (**2a**); △, Me α-D-*ribo*-3-OG (**3a**).

Me α-D-*arabino*-3-OG (**2a**), when maintained in pyridine-$d_5$, changed into **3a**, apparently through **9a**. During this process, the formation of **1a** was again observed (Fig. 2), though its amount never exceeded 8%. The presence of this cycle explains the partial incorporation of deuterium into **2a** in the reaction of **1a** in

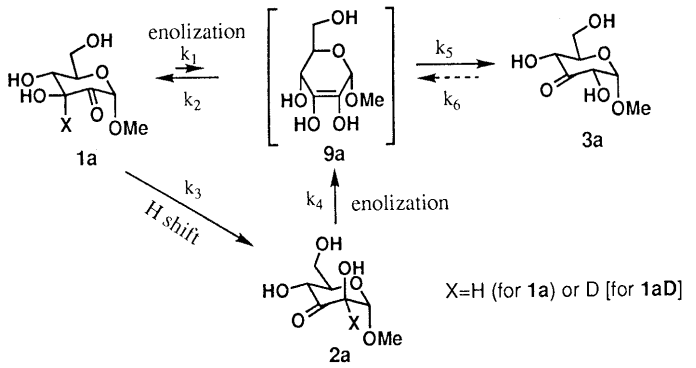


Chart 3

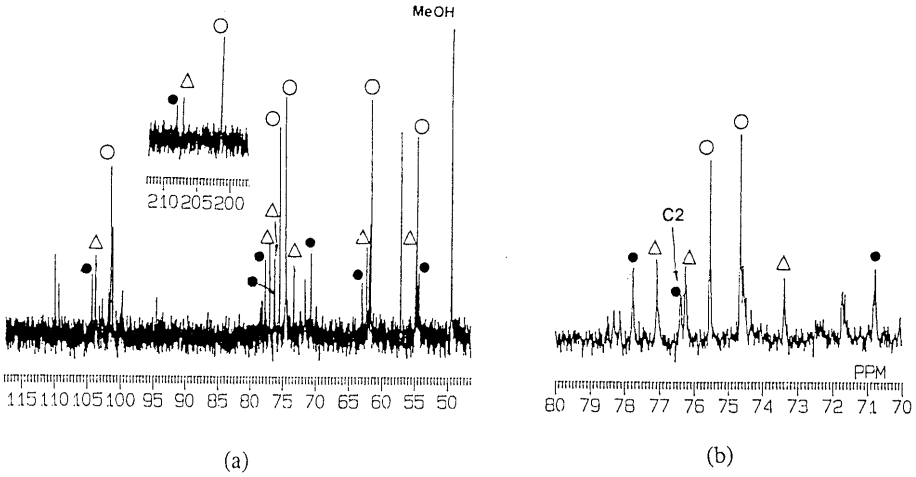


Fig. 3. $^{13}$C-NMR Changes of Me α-D-*arabino*-[3-$^2$H]-2-OG (**1aD**) in Pyridine-$d_5$ (after 48 h)
(a): δ 50—110 region, (b): δ 70—80 region, expanded. ○, Me α-D-*arabino*-2-OG (**1a**); ●, Me α-D-*arabino*-3-OG (**2a**); △, Me α-D-*ribo*-3-OG (**3a**).

pyridine–$D_2O$.

Me α-D-*ribo*-3-OG (**3a**) was stable in pyridine-$d_5$–$D_2O$; it did not incorporate deuterium during 3 weeks at room temperature, indicating that the enolization of **3a** under this condition is very slow and negligible, in extent.

The above lines of evidence revealed that the isomerization of **1a** in pyridine solution proceeds through the paths shown in Chart 3.

Rearrangement of the 3-deuterio derivative (**1a**D) (for the synthesis, see Experimental) in pyridine-$d_5$ revealed that the deuteride shift was slower than the hydride shift, so isomerization through the enediol intermediate (**9a**) predominated for this compound. However, the spectrum during the first 14 h indicated that C-2 of **2a** in the mixture contained more than 30% of deuterium, and this amount gradually decreased (thus increasing the peak intensity of C-2 in **2a**; Fig. 3 indicates the spectrum after 48 h).

The above data clearly indicate that the rearrangement of **1a** in pyridine proceeds mainly through a hydride shift, but with competition from the enolization mechanism: the former predominates for the 3-H derivative and the latter predominates for the 3-D derivative, suggesting retardation of the deuteride shift (see also below).

**Kinetic Studies** Assuming the reaction follows the paths in Chart 3, the rate constant of each step was evaluated from the product distribution in the medium by the use of the NONLIN program[9] (Fig. 4, see also Appendix) to obtain the following values: $k_1 = 0.2 \pm 0.5$, $k_2 = 3.5 \pm 3.3$, $k_3 = 3.7 \pm 0.6$, $k_4 = 1.7 \pm 0.4$, and $k_5 = 9.0 \pm 7.8$ ($\times 10^{-2}$ h$^{-1}$).

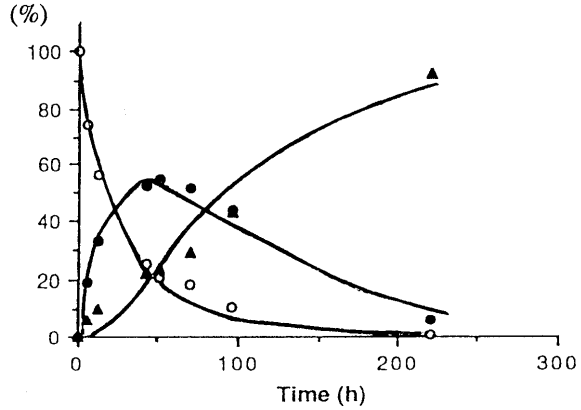


Fig. 4. Changes of Me α-D-*arabino*-2-OG (**1a**) in Pyridine-$d_5$
○, Me α-D-*arabino*-2-OG (**1a**); ●, Me α-D-*arabino*-3-OG (**2a**); ▲, Me α-D-*ribo*-3-OG (**3a**); Observed values: —, Calcd values by a NONLIN programme.

Although the values for $k_1$, $k_2$, and $k_5$ are not very reliable because of large standard deviations, the results show that the hydride shift is the major path in the initial reaction of **1a**, since $k_3/k_1$ is *ca.* 18. On the other hand, $k_4/k_1$ (=8) indicates that the enolization of **2a** is more significant than that of **1a**. Rate constants $k_2$, $k_4$, and $k_5$ are comparable to $k_3$, whereas $k$'s of the other paths, such as enolization of **3a** ($k_6$), under this condition are too small

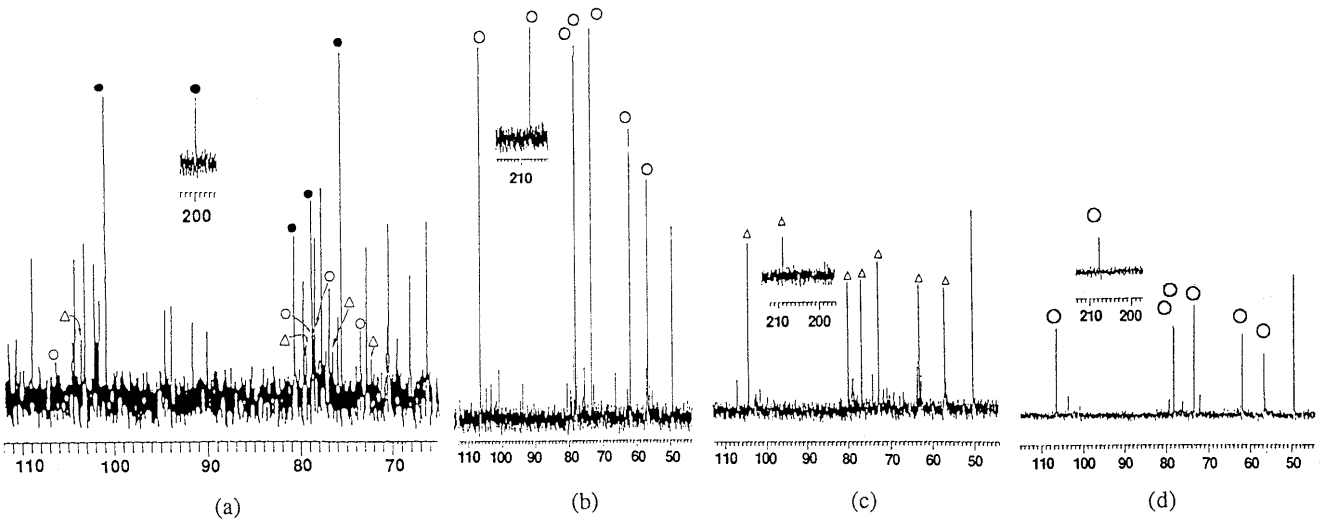


Fig. 5. $^{13}$C-NMR Changes of Me β-D-*arabino*-2-OG (**1b**) and Me β-D-*arabino*-3-OG (**2b**) in Pyridine-$d_5$

(a): from **1b**, after 6 h, (b): from **1b**, after 10 d, (c): from **2b**, after 20 min, (d): from **2b**, after 16 h. ●, Me β-D-*arabino*-2-OG (**1b**); △, Me β-D-*arabino*-3-OG (**2b**); ○, Me β-D-*ribo*-3-OG (**3b**).

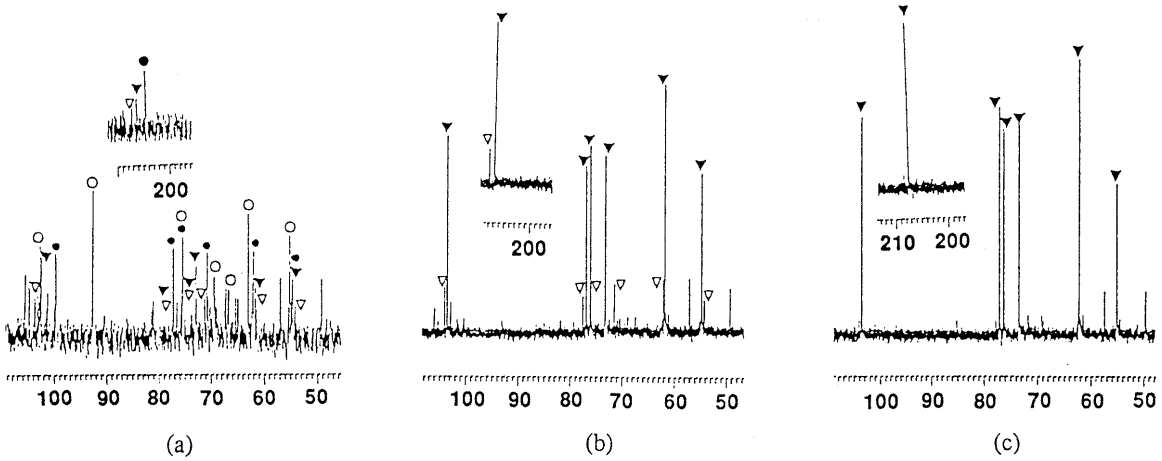


Fig. 6. $^{13}$C-NMR Changes of Me α-D-*ribo*-2-OG (**4**) in Pyridine-$d_5$

(a): after 30 min, (b): after 4.5 h, (c): after 16 h. ●, Me α-D-*ribo*-2-OG (**4**) (oxo form); ○, Me β-D-*ribo*-2-OG (**4**) (hydrate form); ▽, Me α-D-*arabino*-3-OG (**2a**); ▼, Me β-D-*ribo*-3-OG (**3a**).

to be observed, thus being negligible. The evidence shows that, when $k_3$ becomes sufficiently small, as in **1a**D, $k_1$ will become comparable to it, and thus should not be neglected. Rough calculations suggested that $k_3(H)/k_3(D)$ was, at least, larger than 5.

The results also suggest that, if the enolization step ($k_6$) of **3a** to **9a** is not negligible (in other words, increase in the concentration of the enediol intermediate), irreversible change of **9a**, if it occurs, will be significant in the overall reactions. An example of such a case will be shown below.

**Me β-D-*arabino*-2-OG (1b)** A similar hydride shift was found for **1b** in pyridine-$d_5$. The initial product was identified as Me β-D-*arabino*-3-OG (**2b**), which then epimerized into Me β-D-*ribo*-3-OG (**3b**). In this isomerization reaction, however, **3b** was always observed predominantly over **2b**, indicating that the enolization steps (**1b** to **9b**, **2b** to **9b**) are more significant than those in the isomerization of **1a**. In fact, Me β-D-*arabino*-3-OG (**2b**) rapidly isomerized into **3b**, showing only the peaks assignable to **3b** after 16 h (Fig. 5). Me β-D-*ribo*-3-OG (**3b**) was stable under the same conditions for more than 3 weeks.

**Me α-D-*ribo*-2-OG (4)** Me α-D-*ribo*-2-OG (**4**) was far more unstable than **1a**. After 30 min in pyridine-$d_5$, it already showed new peaks attributable to the rearranged products, **2a** and **3a**, together with the oxo and hydrate forms of **4** (**4**-oxo and **4**-hydrate). After 4.5 h, the only peaks were those of **2a** and **3a**, and after 16 h, only those of **3a** (Fig. 6).

In order to check if this rearrangement involves the hydride shift of 3β-H to the 2β position, changes in pyridine-$d_5$–$D_2O$ were examined. When **4** was dissolved in pyridine-$d_5$–$D_2O$, the solution contained only the hydrate (**4**-hydrate), but after 2 h it was a mixture of the oxo form (**4**-oxo) and the hydrate form (**4**-hydrate) in a ratio of 5 : 2, and then the rearrangement occurred from the oxo-form. After 18 h, the spectrum showed the formation of **2a** and **3a** (**2a** > **3a**) with a little **1a** (Fig. 7). Regarding the newly formed **2a** and **3a**, C-2 in **2a** was deuterated almost completely, while that in **3a** remained undeuterated, showing that 2β-H in **3a** is the result of hydride shift from 3β-H of **4**.

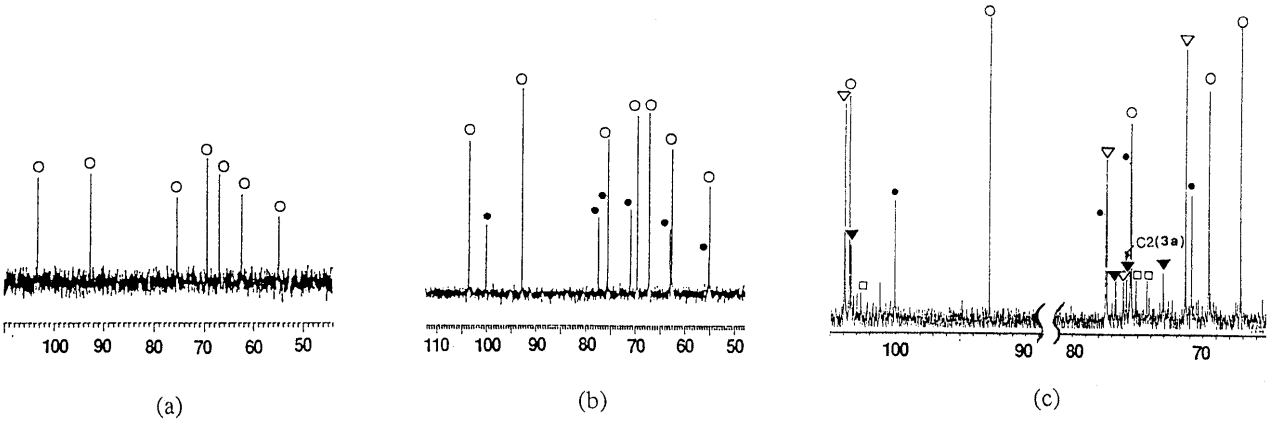


Fig. 7. $^{13}$C-NMR Changes of Me α-D-*ribo*-2-OG (**4**) in Pyridine-$d_5$-$D_2O$

(a): after 5 min, (b); after 2 h, (c): after 18 h. ●, Me α-D-*ribo*-2-OG (**4**) (oxo form); ○, Me α-D-*ribo*-2-OG (**4**) (hydrate form); ▽, Me α-D-*arabino*-3-OG (**2a**); ▼, Me α-D-*ribo*-3-OG (**3a**); □, Me α-D-*arabino*-2-OG (**1a**).

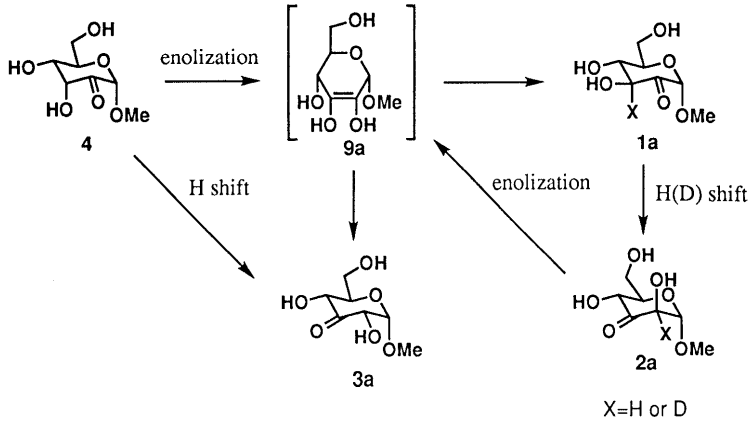


Chart 4

Since **1a** in this reaction is produced from **4** through enolization, its C-3 is deuterated and since it rearranges to **2a** through a deuteride shift, the resulting **2a** incorporates deuterium. The enolization rate of **2a**(D) is presumed to be sufficiently slower than that of **2a**(H) that its intermediary formation can be clearly observed. This process finally gives **3a**, which accordingly is deuterated at C-2. Therefore, on continuation of the reaction, the relative peak intensity of C-2 in **3a** gradually decreased, though the total amount of **3a** increased.

The rearrangement rate of **4** in pyridine-$d_5$ is *ca.* 10 times faster than that in pyridine-$d_5$–$D_2O$. This may be rationalized as follows: (1) in pyridine–$D_2O$, the ratio of the hydrate form increased, thus reducing the concentration of the oxo form, from which the isomerization takes place, and (2) in pyridine–$D_2O$, the deuterated compound is produced as an intermediate, which retards the reaction thereafter.

The above results show that 3-equatorial H can also undergo the hydride shift to give directly the product bearing 2-equatorial OH.

**Changes of Oxoglycosides Bearing an Axial Hydroxyl Group at C-4. Me α-D-*lyxo*-2-OG (5)** Me α-D-*lyxo*-2-OG (**5**), on storage in pyridine-$d_5$ at 37 °C, disappeared after 2 d, changing into a different species. The product possesses neither an OMe nor an anomeric carbon signal, but exhibited olefinic carbon signals at $\delta$ 136.6 (s) and 147.8 (d), together with a carbonyl carbon signal at $\delta$ 189.0 (s) (Fig. 8). The H–C correlation spectroscopy (COSY) spectrum of this product showed a correlation between the carbon signal at $\delta$ 147.8 and the proton signal at $\delta$ 7.79, as well as the presence of the partial structure –CH(O–)–CH(O–)–$CH_2$OH. Therefore it was assigned as **11**, which would be produced from the intermediary enediol (**10**) by the conjugate elimination of methanol.

In support of this, Me α-D-*xylo*-3-OG (**6**), on storage in pyridine-$d_5$ at 27 °C, changed into the same product (**11**) after 11 d.

In the above reactions, epimerization of the 4-OH group was not observed, indicating that enolization of the C-3 carbonyl toward C-4 does not occur and it is reversibly enolizable only toward C-2. This easy reversible enolization and elimination of methanol from 2- or 3-oxoglycosides bearing 4-axial OH are presumed to be due to increased stability, and consequently concentration, of the 2,3-enediol (**10**) in the medium, because this species apparently has smaller $A^{(1,2)}$ strain[10] than that in the corresponding 2,3-enediol with 4-equatorial OH (such as **9a**). More detailed analysis is shown in the following examples.

**Me α-D-*xylo*-2-OG (7)** The transformation of **7** in pyridine-$d_5$ at 27 °C is relatively rapid (Fig. 9). After 17 h, peaks of **7** disappeared and those corresponding to four compounds appeared. They were assigned as **5**, **6**, **8**, and

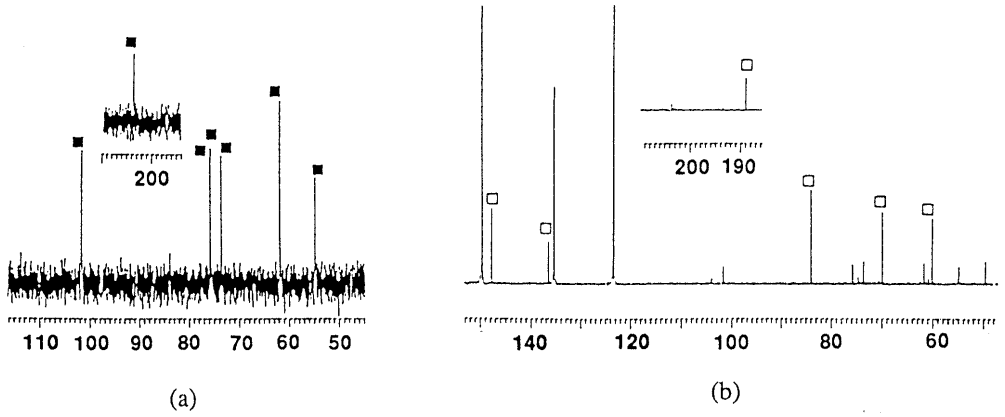


Fig. 8. $^{13}$C-NMR Changes of Me α-D-*lyxo*-2-OG (**5**) in Pyridine-$d_5$
(a): after 1 h, (b): after 35 h. ■, Me α-D-*lyxo*-2-OG (**5**); □, **11**.

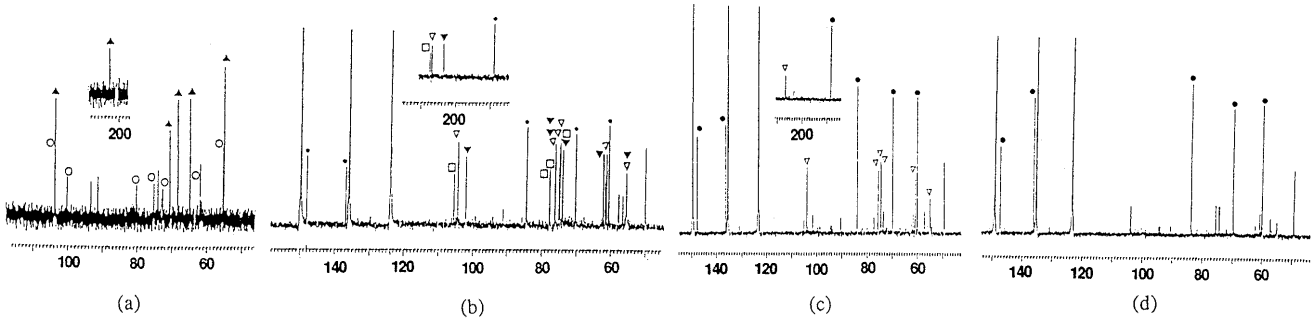


Fig. 9. $^{13}$C-NMR Changes of Me α-D-*xylo*-2-OG (**7**) in Pyridine-$d_5$
(a): after 1 h, (b): after 17 h, (c): after 3 d, (d): after one week. ●, **11**; ○, Me α-D-*xylo*-2-OG (**7**) (hydrate form); ▲, Me α-D-*xylo*-2-OG (**7**) (oxo form); ▼, Me α-D-*lyxo*-2-OG (**5**); □, Me α-D-*lyxo*-3-OG (**8**); ▽, Me α-D-*xylo*-3-OG (**6**).

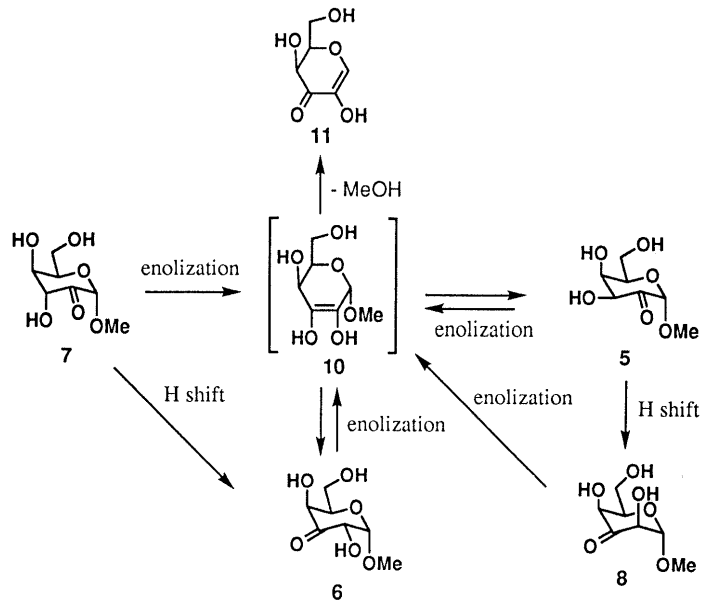


Chart 5

**11** on the basis of comparisons with the spectra of authentic samples. After 3 d, **5** and **8** disappeared, leaving **6** and **11**, and after a week, there remained only the peaks of **11**. The initial formation of **5** and **6** from **7** can be explained by either hydride shift and/or enolization mechanisms as discussed above. Compound **8** should be the hydride shift product from **5**. All of these species are enolizable to the enediol (**10**), which liberates methanol by conjugate elimination, giving rise to **11**. Enolization of **6** to **10** should be easier than that of **3a** to **9a**, since very little of **6** remained in the solution after a week.

**Further Changes of Me α- and β-*ribo*-3-OG (3a, 3b) in Pyridine-$d_5$** Although 3-oxo derivatives of *ribo*-configuration (**3a**, **3b**) were stable in pyridine-$d_5$ for over a month as described above, slow but distinct change was observed on prolonged standing in the same solvent (Fig.

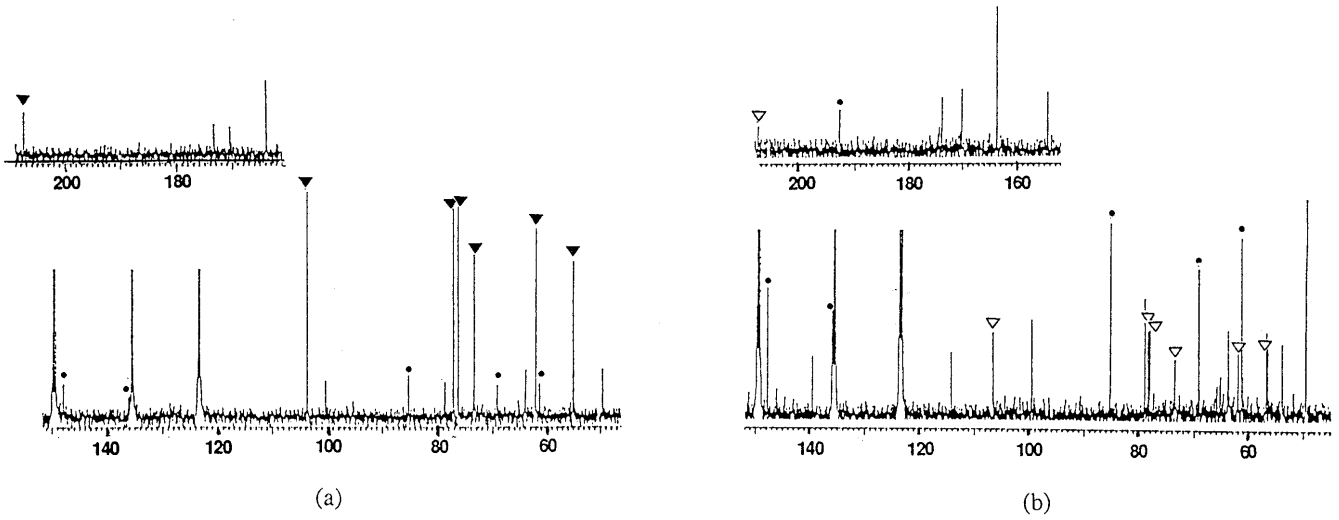


Fig. 10. $^{13}$C-NMR Changes of Me α-D-*ribo*-3-OG (**3a**) and Me β-D-*ribo*-3-OG (**3b**) in Pyridine-$d_5$
(a): **3a** after 90 d, (b): **3b** after 78 d. ●, **12**; ▼, Me α-D-*ribo*-3-OG (**3a**); ▽, Me β-D-*ribo*-3-OG (**3b**).

10). The change was similar to that discussed for oxoglycosides with 4-axial OH. Me α-D-*ribo*-3-OG (**3a**) gave 20—30% of a demethanolated product after 3 months, while **3b** changed more rapidly, gradually giving the same product after a month. The structure of the product was assigned as **12** on the basis of $^{13}$C-NMR spectral analogy with the spectrum of **11**.

Since **12** is formed from the enediols, **9a** and **9b**, the above results indicate that the reverse enolizations (**3a** to **9a**, **3b** to **9b**) obviously proceed, though the reaction is very slow at 27 °C in pyridine-$d_5$.

## Conclusion

All 2-oxoglycosides were, more or less, unstable in pyridine-$d_5$ and isomerized into 3-oxoglycosides. Although the products differ depending on the starting materials, hydride shift is the major path for the initial reaction of all 2-oxoglycosides, typical paths being summarized in Chart 3. The hydride shift was over 10 times greater than the enolization for oxoglycosides of *arabino*-configuration. Intermediary 3-oxoglycosides of unstable configuration further isomerized, through an enolization mechanism, to 3-oxoglycosides of *ribo*-configuration. For oxoglycosides bearing axial OH at C-4, the enolization step becomes significant. Thus, the conjugate elimination of methanol from the 2,3-enediol intermediate to produce irreversibly a compound of diosphenol structure is the major reaction path.

### Experimental

**$^{13}$C-NMR Spectra** The spectra were measured on a JEOL GX-400 (100 MHz) or GX-500 (125 MHz) spectrometer with tetramethylsilane as an internal standard and the chemical shifts are given in δ values.

**Reaction of Oxoglycosides in Pyridine (General Procedure)** (1) In Pyridine-$d_5$: Oxoglycosides (15—40 mg) were dissolved in pyridine-$d_5$ (0.6 ml) and the mixture was kept standing at 27 °C, during which time the $^{13}$C-NMR spectrum was taken periodically. Identification of the compound in the solution was achieved by comparisons of the spectra with those of authentic specimens[1] in the same solvent. The ratio of the components was roughly determined from the intensity ratio of anomeric carbons, which is roughly proportional to the component ratio.[11]

(2) In Pyridine-$d_5$–$D_2O$: Oxoglycosides (10—40 mg) were kept in $D_2O$ for 10 min, then lyophilized. The residue was dissolved in pyridine-$d_5$ (0.6 ml) containing $D_2O$ (2 drops) and the solution was kept at 27 °C with periodic monitoring of the $^{13}$C-NMR spectrum as above.

**Reaction of Me α-D-*lyxo*-2-OG (6a) at 37 °C** Compound **6a** was kept in pyridine-$d_5$ at 37 °C and treated as described in the general procedure. The $^1$H, $^{13}$C, and C–H COSY spectra after 35 h were measured *in situ*.

**Methyl α-D-*arabino*-3-Deuterio-hexopyranosid-2-ulose (1aD)** (1) A mixture of Me β-D-*ribo*-3-OG[6] (**3b**, 0.8 g) and $NaBD_4$ (0.3 mol eq, 53 mg) in MeOH (50 ml) was stirred at room temperature for 1 h. The mixture was neutralized with 1 N HCl and concentrated to dryness. The residue was dissolved in MeOH and then concentrated. This procedure was repeated 3—5 times to remove completely borate complexes. The residue was adsorbed on a silica gel column, and the column was eluted with $CHCl_3$–MeOH (3 : 1) to yield the [3-$^2$H]-derivative (0.75 g, 93%) as a 1 : 1 mixture of Me β-D-Glc and Me β-D-All [by gas chromatgraphic (GC) analysis as the trimethylsilyl (TMS) derivative].

(2) The above residue was dissolved in 6% HCl–MeOH and heated under reflux for 5 h, then concentrated to dryness. Although the product is a mixture of four compounds (Me α-, and β-D-All, Me α- and β-D-Glc), it showed two spots on thin-layer chromatography (TLC), corresponding to Me D-All and Me D-Glc, which were separated by flash chromatography on silica gel ($CHCl_3$ : MeOH = 5 : 1) to yield a mixture of Me D-Glc (0.36 g, α : β = 7 : 3 by GC analysis as a TMS derivative).

(3) This mixture (0.35 g), 1,1-dimethoxytoluene (1 ml), and a catalytic amount of *p*-TsOH (2 mg) in dimethylformamide (DMF) (5 ml) were heated at 60—70 °C for 6 h. The reaction mixture was poured into dilute aqueous $NaHCO_3$ and extracted with AcOEt. The dried extract, on evaporation of the solvent, gave a gummy residue, which was purified by flash chromatography (hexane–AcOEt) to give Me 4,6-*O*-benzylidene-α-D-3-deuterio-glucopyranoside (**13**) (0.3 g) as colorless prisms (mp 165—167 °C). $^{13}$C-NMR ($CDCl_3$): 131.7, 129.1, 128.2, 126.3 (Ph), 101.8 ($PhCHO_2$), 99.8 (C1), 72.3 (C2), 80.8 (C4), 62.3 (C5), 68.9 (C6), 55.4 (OMe).

(4) A mixture of **13** (270 mg), $(Bu_3Sn)_2O$ (1.7 g, 3 mol eq), and molecular sieves 3 Å (2 g) in toluene (30 ml) was heated under reflux for 5 h. Then the mixture was ice-cooled and $Br_2$ (*ca.* 3 mol eq) was added dropwise until a faint color persisted, and the reaction mixture was worked up as described in ref. 1 to yield the 2-oxo derivative **14** (244 mg, 91%).

(5) The 2-oxo derivative **14** (120 mg) in 50% AcOH was heated at 100 °C for 15 min. The mixture was diluted with water, then lyophilized. Chromatography of the residue on silica gel ($CHCl_3$ : MeOH = 3 : 1) gave **1aD** (72 mg, 88%) as a colorless gum. $^{13}$C-NMR: 201.6 (C2). 101.5 (C1), 75.5 (C4), 61.8 (C6), 54.7 (OMe). HR-MS: Calcd for $C_7H_{11}DO_6$ ($M^+$): 193.0696. Found: 193.0730.

**Appendix (Evaluation of *k*'s)** The product distribution in the medium was roughly calculated from the C-1 peak intensities of each component (Fig. 4). Assuming the reaction paths of **1a** to be as represented by model **1** (Chart 3), the rate constants (*k*'s) were calculated from Eq. 1—4, where

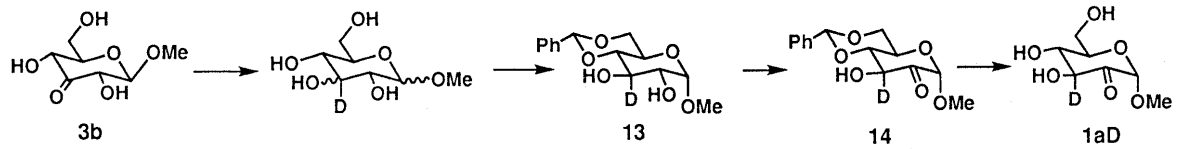


Chart 6

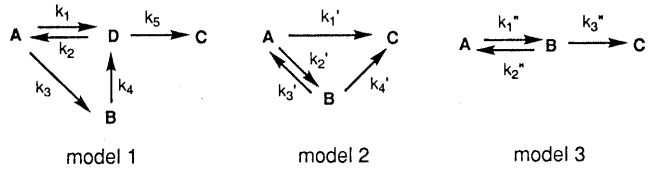


Chart 7

[A], [B], [C], and [D] are concentrations of **1a**, **2a**, **3a**, and **9a**, respectively.

$$d[A]/dt = k_2[D] - (k_1 + k_3)[A] \quad (1)$$

$$d[B]/dt = k_3[A] - k_4[B] \quad (2)$$

$$d[C]/dt = k_5[D] \quad (3)$$

$$d[D]/dt = k_1[A] + k_4[B] - (k_2 + k_5)[D] \quad (4)$$

Since [D] was not observable, $k$'s were obtained by the following procedures. Firstly, model 1 was transformed into model 2, where $k'_2 = k_3$, $k'_3 + k'_4 = k_4$, and $k'_1$ represents the path through the direct enolization of **1a**. Calculations by use of the NONLIN program[9] gave the following values: $k'_1 = 0.1 \pm 0.2$, $k'_2 = 3.7 \pm 0.5$, $k'_3 = 0.5 \pm 0.02$, and $k'_4 = 1.2 \pm 0.2$ ($\times 10^{-2}\,h^{-1}$). Therefore $k_3 = 3.7 \pm 0.5$ and $k_4 = 1.7 \pm 0.2$ ($\times 10^{-2}\,h^{-1}$); $k_1$ was very small and the value obtained was not reliable (C.V. = 200%).

When we neglect $k_1$ (as model 3), calculations gave values that agreed with the experimental results, $k''_1 = 3.8 \pm 0.4$, $k''_2 = 0.5 \pm 0.2$, and $k''_3 = 1.2 \pm 0.1$ ($\times 10^{-2}\,h^{-1}$), with C.V.'s of 11%, 47%, and 8%, respectively. Rate constants $k_3$ and $k_4$ were again calculated as $3.8 \pm 0.4$ ($\times 10^{-2}\,h^{-1}$) and $1.7 \pm 0.4$ ($\times 10^{-2}\,h^{-1}$), respectively, since $k_3 = k''_1$ and $k_4 = k''_2 + k''_3$.

Although the rate constants $k_3$ (hydride shift of **1a**) and $k_4$ (enolization of **2a**) were thus obtained, $k_1$, $k_2$, and $k_5$ were not directly obtained, even if the above values were inserted to Eq. 1; calculations gave several sets of these values, all of which were consistent with the experimental results. However, the isomerization experiment starting from **2a** gave further information: that is, though **1a** was formed as one of the intermediates, its concentration never exceeded 8% (see text). Thus, calculations, for example, with two sets of $k$'s [set 1: $k_1 = 0.3$, $k_2 = 1.8$, $k_5 = 5.0$; set 2: $k_1 = 0.2$, $k_2 = 3.5$, $k_5 = 9.0$ ($\times 10^{-2}\,h^{-1}$)] revealed that the latter set was more reliable, because for the former set the maximum concentration of intermediary **1a** (A) was 20% and for the latter set it was 6.5%. Thus, the following values were adopted as the most reliable ones for $k$'s of each step in Chart 3: $k_1 = 0.2 \pm 0.5$, $k_2 = 3.5 \pm 3.3$, $k_3 = 3.7 \pm 0.6$, $k_4 = 1.7 \pm 0.4$, and $k_5 = 9.0 \pm 7.8$ ($\times 10^{-2}\,h^{-1}$).

**References and Notes**

1) Part XXVIII of Utilization of Sugars in Organic Synthesis. Part XXVII: Liu H.-M., Sato Y., Tsuda Y., *Chem. Pharm. Bull.*, **41**, 491—501 (1993).
2) A part of this work was presented as a communication: Tsuda Y., Liu H.-M., *Chem. Pharm. Bull.*, **40**, 1975—1977 (1992).
3) Present address: *Department of Chemistry, Zhengzhou University, Zhengzhou 450052, P. R. China.*
4) *a*) Matsuhashi M., Strominger J. L., *Methods Enzymol.*, **8**, 317—323 (1966); *b*) Gabriel O., *Adv. Chem. Ser.*, **117**, 387—410 (1973); *c*) Baute R., Baute M.-A., Deffieux G., *Phytochemistry*, **26**, 1395—1397 (1987); *d*) Saito K., Nick J. A., Loewus F. A., *Plant Physiol.*, **94**, 1496—1500 (1990).
5) Theander O., *Acta Chem. Scand.*, **12**, 1887—1896 (1958).
6) Tsuda Y., Hanajima M., Matsuhira N., Okuno Y., Kanemitsu K., *Chem. Pharm. Bull.*, **37**, 2344—2350 (1989).
7) Abbreviations: Me = methyl, OG = hexopyranosidulose, Glc = glucopyranoside, All = allopyranoside. For example, Me α-D-*ribo*-2-OG (**1a**) represents methyl α-D-*ribo*-hexopyranosid-2-ulose.
8) The enolization process was accelerated under this condition.
9) Metzler C.M., "NONLIN, a computer program for parameter estimation in nonlinear situations," Technical Report, 729/69/7297/005, Upjohn Co., Kalamazoo, Mich.
10) Johnson F., Malhotra S. K., *J. Am. Chem. Soc.*, **87**, 5492—5493 (1965).
11) Tsuda Y., Haque M. E., Yoshimoto K., *Chem. Pharm. Bull.*, **31**, 1612—1624 (1983).